

1 **Cyclodextrin polymers as passive sampling materials for lipophilic marine toxins in**

2 **Prorocentrum lima cultures and a Dinophysis sacculus bloom in the NW**

3 **Mediterranean Sea**

4

5 Mònica Campàs^{1,*}, Maria Rambla-Alegre¹, Charlotta Wirén¹, Carles Alcaraz¹, María Rey¹, Anna

6 Safont¹, Jorge Diogène¹, Mabel Torréns², Alex Fragoso²

7

8 ¹ IRTA, Ctra Poble Nou km 5.5, 43540 Sant Carles de la Ràpita, Spain

9 ² Departament d'Enginyeria Química, Universitat Rovira i Virgili, Avinguda Països Catalans 26,

10 43007 Tarragona, Spain

11 monica.campas@irta.cat

12

13 **Abstract**

14 Cyclodextrins, cyclic oligomers that form a conical structure with an internal cavity, are proposed

15 as new and sustainable materials for passive sampling of lipophilic marine toxins. Two

16 applicability scenarios have been tested. First, disks containing β -cyclodextrin-hexamethylene

17 diisocyanate (β -CD-HDI) and β -cyclodextrin-epichlorohydrin (β -CD-EPI) polymers were

18 immersed in *Prorocentrum lima* cultures for different days (2, 12 and 40). LC-MS/MS analysis

19 showed capture of free okadaic acid (OA) and dinophysistoxin-1 (DTX1) by cyclodextrins at

20 contents that increased with immersion time. Cyclodextrins resulted more efficient in capturing

21 DTX1 than OA. In a second experiment, disks containing β -CD-HDI, β -CD-EPI, γ -CD-HDI and γ -CD-

22 EPI were deployed in harbor waters of El Masnou (NW Mediterranean Sea) during a *Dinophysis*

23 *sacculus* bloom in February 2020. Free OA and pectenotoxin-2 (PTX2) were captured by

24 cyclodextrins. Toxin contents were higher at sampling points and sampling weeks with higher
25 *D. sacculus* cell abundance. In this case, PTX2 capture with cyclodextrins was more efficient than
26 OA capture. Therefore, cyclodextrins have provided information regarding the toxin profile of a
27 *P. lima* strain and the spatial and temporal dynamics of a *D. sacculus* bloom, proven efficient as
28 passive sampling materials for environmental monitoring.

29 **Keywords**

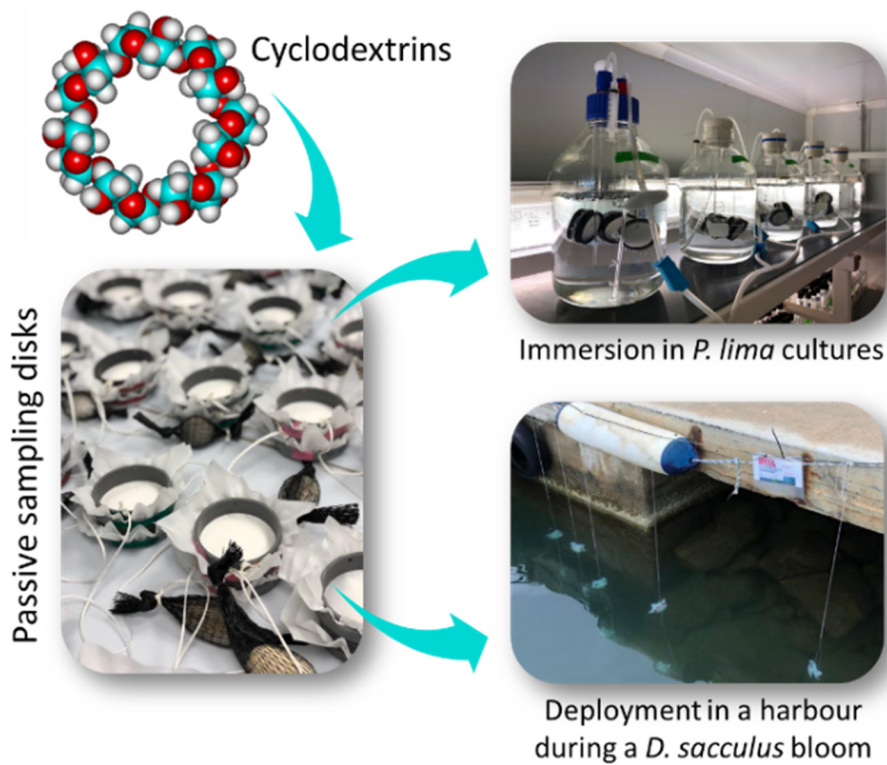
30 Cyclodextrin, okadaic acid (OA), dinophysistoxin-1 (DTX1), pectenotoxin-2 (PTX2), *Prorocentrum*
31 *lima*, *Dinophysis sacculus*.

32

33

34

35 **Graphical abstract**



36

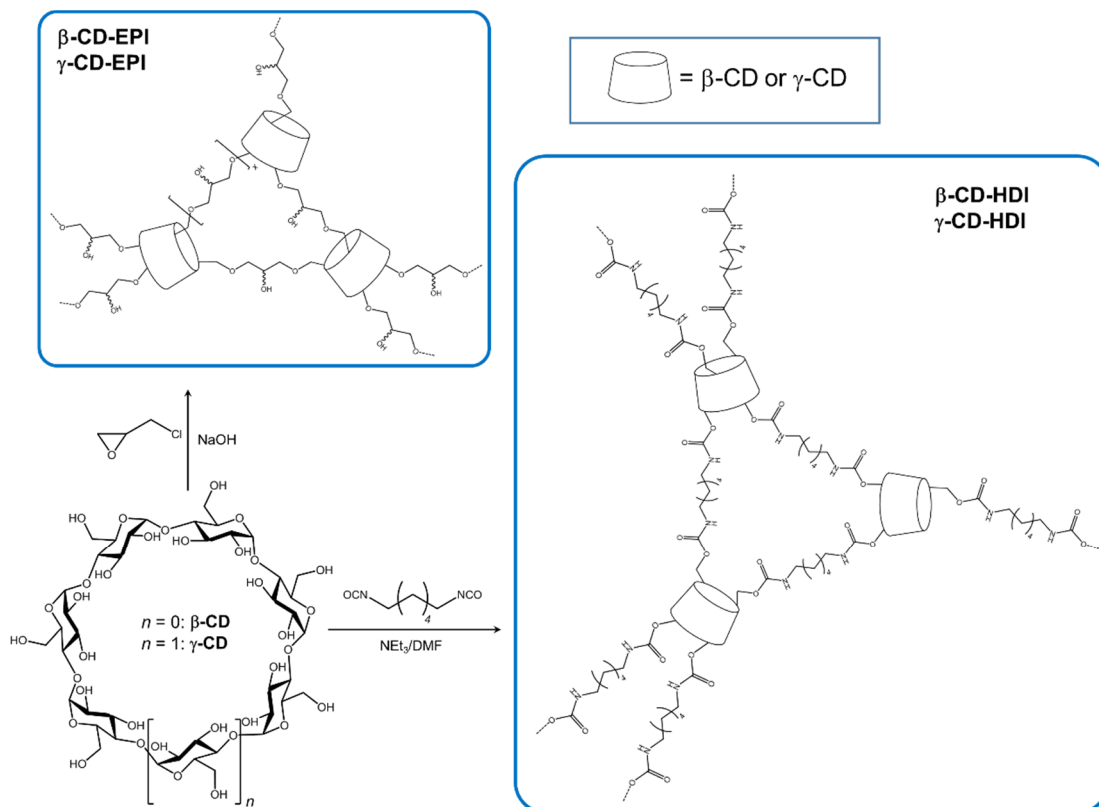
37 **1. Introduction**

38 Harmful algal blooms (HABs) are increasing in geographical expansion, frequency and severity,
39 some of the possible reasons being ocean warming, eutrophication and globalization (Wells et
40 al., 2020). HABs represent a threat for food safety and consumers, since toxins produced by toxic
41 microalgae are accumulated by shellfish and fish. Regarding shellfish safety, monitoring
42 programs involve sampling of shellfish for analysis of marine toxins as well sampling of seawater
43 for phytoplankton identification and counting. Early warning of HABs and shellfish contamination
44 would be a useful approach to facilitate management and protect human health.

45 Solid-phase adsorption toxin tracking (SPATT) was conceived by MacKenzie in 2004 (MacKenzie
46 et al., 2004). The technique involves the passive adsorption of toxins on porous synthetic resins
47 for the subsequent extraction and analysis. These resins are encased into different types of
48 frames and are deployed into the water column, where they can adsorb the toxins released by
49 toxic microalgae. Passive samplers have been proposed as an early warning tool to forecast
50 shellfish contamination or at least as complementary tool in monitoring programs. The main
51 advantages of passive samplers are simplicity, low cost, low matrix effects when analyzing the
52 resins, spatially and temporally integrated responses, and accumulative capacity. However, some
53 issues still need to be resolved, such as optimal deployment times, saturation limits, lack of
54 calibration and standardization, and the insufficient knowledge about the correlation with toxin
55 contents in shellfish. Additionally, a major limitation is that they allow the monitoring of
56 dissolved toxins only. Nevertheless, passive samplers already have an undeniable application in
57 environmental monitoring and research, since they can provide information on HABs such as
58 geographical and temporal distribution, environmental persistence and toxin dynamics.

59 Diaion® HP-20 has been the adsorbent substrate most commonly used in passive samplers (Roué
60 et al., 2018) both in microalgae cultures (Fux et al., 2008; Li et al., 2011; Kudela, 2017) and field
61 studies (MacKenzie et al., 2004; Zendong et al., 2015; Kudela, 2017). Unlike this resin, which
62 adsorbs toxins, cyclodextrins (CDs) can capture organic compounds by supramolecular

63 interactions, which may result in different affinity, kinetics and saturation behaviors.
64 Cyclodextrins are cyclic α -1 \rightarrow 4-linked glucose oligomers that form a conical structure with an
65 essentially hydrophobic internal cavity filled with disordered water molecules and two external
66 hydrophilic rims decorated with hydroxyl groups. The number of glucose units in the most
67 common cyclodextrins, 6 in α -CD, 7 in β -CD and 8 in γ -CD, dictates the size of the cavity, which
68 allows the inclusion of a variety of organic molecules of appropriate size, shape and polarity
69 (Villalonga et al., 2007). They have been exploited in different fields, such as in targeted therapy
70 as drug carriers (Ramirez et al., 2006a, 2006b, 2007), and in biosensors for electrode surface
71 modification and signal amplification (Ortiz et al., 2011a, 2011b, 2011c, 2011d, 2012, 2014; Wajs
72 et al., 2014, 2016). Nevertheless, until now they had never been used for marine toxin tracking.
73 In this work, several insoluble cyclodextrin polymers (β -cyclodextrin-hexamethylene
74 diisocyanate (β -CD-HDI), β -cyclodextrin-epichlorohydrin (β -CD-EPI), γ -cyclodextrin-
75 hexamethylene diisocyanate (γ -CD-HDI) and γ -cyclodextrin-epichlorohydrin (γ -CD-EPI)) (Fig. 1)
76 have been immersed in *Prorocentrum lima* cultures and deployed in harbor waters during a
77 *Dinophysis sacculus* bloom for their evaluation as new and sustainable passive sampling
78 materials. The commercial Diaion® HP-20 has been used as a control. Results have been useful
79 to obtain information about the toxin profile of the *P. lima* strain and to elucidate the toxin
80 production, development and dynamics of the *D. sacculus* HAB.



81

82 **Figure 1.** Schematic representations of β -CD-HDI, β -CD-EPI, γ -CD-HDI and γ -CD-EPI and their syntheses
 83 from native β -CD and γ -CD.

84 2. Materials and methods

85 2.1. Reagents and materials

86 β -CD-HDI and γ -CD-HDI were synthesized by crosslinking the native dried CDs with
 87 hexamethylene diisocyanate (1:7 and 1:8 molar ratio, respectively) in dimethylformamide
 88 containing triethylamine (Mohamed et al., 2011). β -CD-EPI and γ -CD-EPI were prepared by
 89 reaction of the native CDs with epichlorohydrin (1:14 and 1:16 molar ratio, respectively) in NaOH
 90 (Crini et al., 1998) (Fig. 1). The products were purified by Soxhlet extraction with EtOH and water.
 91 Diaion® HP-20 Supelco resin was obtained from VidraFoc (Barcelona, Spain). Certified reference
 92 material of okadaic acid (OA) (15.56 $\mu\text{g mL}^{-1}$ in MeOH) was obtained from CIFGA (Lugo, Spain).
 93 Dinophysistoxin-1 (DTX1) (8.52 $\mu\text{g mL}^{-1}$ in MeOH) and pectenotoxin-2 (PTX2) (4.40 $\mu\text{g mL}^{-1}$ in
 94 MeOH) were obtained from the National Research Council of Canada (NRC, Halifax, Canada).

95 Passive sampling disks were constructed by placing 1 g (cultures) or 10 g (harbor) of β -CD-HDI,
96 β -CD-EPI, γ -CD-HDI, γ -CD-EPI or Diaion® HP-20 between two layers of 1 μ m nylon mesh (Sefar
97 Maissa S.A.U., Cardedeu, Barcelona, Spain), clipped between two cylindrical PVC rings (4-cm
98 diameter for immersion in cultures and 7-cm diameter for deployment in a harbor) (Fig. 1SA).
99 The passive sampling disks to be deployed in the harbor were provided with a counterweight to
100 ensure stability. Cyclodextrins and resin were activated by soaking the disks in MeOH for 15 min
101 and rinsing them with milli-Q water.

102 **2.2. Immersion of cyclodextrins in *Prorocentrum lima* cultures**

103 Clonal cultures of *P. lima* strain IRTA-SMM-17-47 (GenBank accession number: MW328564) from
104 IRTA collection were grown in modified ES medium (Provasoli, 1968), first in Nunclon™ cell
105 culture polystyrene flasks (Thermo Fisher Scientific) and afterwards in glass bottles. Modified ES
106 medium was prepared with sterile aged seawater obtained from L'Ametlla de Mar (Spain),
107 Mediterranean Sea (40.8465° N; 0.77243° E) at 10 m depth, which was passed through an
108 activated carbon-PTFE membrane filter (Thermo Fisher Scientific) and a 0.22- μ m cellulose
109 acetate filter (Merck KGaA, Germany). The salinity was adjusted to 36 with milli-Q water. Cultures
110 were maintained at 24 ± 0.5 °C under a light intensity of $110 \mu\text{mol photons m}^{-2} \text{s}^{-1}$ with a 12:12 h
111 light:dark regime. Passive sampling disks containing of β -CD-HDI, β -CD-EPI or Diaion® HP-20
112 were immersed into *P. lima* cultures (3 disks per glass bottle) at day 0, and collected at day 2, day
113 12 and day 40 (Fig. 1SB) (at the time of the experiment, γ -CD-HDI and γ -CD-EPI were not
114 available). A culture with no passive sampling disks was used as a control to evaluate if their
115 presence had any effect on the culture growth. Two aliquots of each culture were taken every
116 few days, fixed with 3% Lugol's iodine, and cells were counted in duplicate using a Kolkwitz
117 chamber (Hydro-Bios, Altenholz, Germany) under an inverted light microscope (Leica DMIL,
118 Spain). Cultures (~4 L) were harvested at day 40 through vacuum filtration using a 5- μ m nylon
119 mesh (Sefar Maissa S.A.U., Spain).

120 **2.3. Deployment of cyclodextrins in a harbor during a *Dinophysis sacculus* bloom**

121 Two consecutive deployments lasting 7 days (from 14/02/2020 to 21/02/2020, and from
122 21/02/2020 to 28/02/2020) were performed at 5 sampling points of El Masnou harbor (NW
123 Mediterranean Sea) during a *D. sacculus* bloom (Fig. 2S). Passive sampling disks containing of β -
124 CD-HDI, β -CD-EPI, γ -CD-HDI, γ -CD-EPI or Diaion® HP-20 (in duplicate) were deployed at 1.2 m
125 depth and left for 1 week (Fig. 1SC). Phytoplankton cells were counted under an inverted light
126 microscope (Leica DMIL, Spain), following the Utermöhl method (Utermöhl, 1931).

127 **2.4. Toxin extraction**

128 The passive sampling disks were soaked in milli-Q water for 30 min. Afterwards, the embroidery
129 hoop was opened, and the β -CD-HDI, β -CD-EPI, γ -CD-HDI, γ -CD-EPI or Diaion® HP-20 were
130 transferred to beakers and incubated with MeOH (40 mL when using 1 g (cultures) and 80 mL
131 when using 10 g (harbor)) for 2 h. Cyclodextrins and resin were then transferred to low frequency
132 polyvinyl chloride (LPVC) plastic filtration columns containing 1 μ m nylon mesh filters and frits,
133 vacuum was applied with a Vac-Elut SPE vacuum manifold (Varian, Harbor City, CA, USA), and the
134 MeOH was collected. Rinsing was performed with additional MeOH (20-30 mL approx.), which
135 was also collected. The total volume of eluate was evaporated to dryness in a Syncore Buchi
136 (Flawil, Switzerland) and redissolved in 0.5 (when using 1 g) or 4 mL (when using 10 g) of MeOH.
137 *Prorocentrum lima* culture media (0.5 L) were filtered through Empore™ C18 SPE Disks (Supelco,
138 Sigma-Aldrich, Tres Cantos, Madrid, Spain). Disks were first conditioned with 10 mL of MeOH and
139 10 mL of milli-Q water. Then, culture media were loaded, vacuum was applied, and the collected
140 media were discarded. Samples were then eluted with 20 mL of MeOH. *Prorocentrum lima*
141 cultures filters were sonicated 3 times in 150 mL of MeOH for 30 min. The three extracts were
142 joined and centrifuged at 3,000 rpm for 10 min, and the supernatant was kept.
143 To investigate the possible presence of fatty acid acyl esters, alkaline hydrolysis of the extracts
144 was performed the same day of analysis by adding 125 μ L of 2.5 M NaOH in 1.25 mL of extract

145 in a HPLC vial (the same ratio was maintained when hydrolyzing extracts coming from 1 g of
146 cyclodextrin or resin), vortexing for 0.5 min, and heating at 76 °C for 40 min. Samples were then
147 cooled at room temperature, neutralized with 125 µL of 2.5 M HCl, and vortexed for 0.5 min.

148 All extracts were passed through 0.2-µm PTFE syringe filters and stored at -20 °C until LC-MS/MS
149 analysis.

150 **2.4. LC-MS/MS analysis**

151 LC-MS/MS analyses were conducted on a 1200 LC system (Agilent Technologies, Santa Clara, CA)
152 coupled with a 3200 QTRAP triple quadrupole mass spectrometer through a TurboV electrospray
153 ion source (Applied Biosystems, Foster City, CA), using a previously described methodology
154 (García-Altarets et al., 2016; Leonardo et al., 2018). Samples were analyzed on an XBridge BEH C8
155 column, 2.5 µm, 2.1 × 50 mm and an XBridge BEH C8 Prep Guard cartridge, 2.5 µm, 2.1 x 5 mm
156 (Waters, Milford, MA, USA). A binary gradient was programmed with ultrapure milli-Q water
157 (mobile phase A) and 90:10 v:v acetonitrile:water (mobile phase B), both containing 6.7 mM of
158 ammonium hydroxide. Mobile phases were filtered through 0.2-µm nylon membrane filters
159 (Whatman, Springfield Mill, UK). Chromatographic separations were performed at 30 °C using a
160 flow rate of 500 µL min⁻¹. The elution gradient started at 20% B, reached 100% B in 8 min, held
161 for 1 min, then back to 20% B in 1 min and equilibrated for 2 min before the next run started.
162 The injection volume was 10 µL and the auto-sampler was set at 4 °C. A total run time of 12 min
163 was used. Lipophilic toxins were analyzed in both negative (-ESI) and positive (+ESI) mode,
164 selecting two product ions per toxin to allow quantification (the most intense transition) and
165 confirmation (the second intense transitions). Identification was supported by toxin retention
166 time and multiple reaction monitoring (MRM) ion ratios. Monitored transitions of the detected
167 toxins were 803.5>255.0 *m/z* (MRM1) and 803.5>113.0 *m/z* (MRM2) for OA, 817.5>255.2 *m/z*
168 (MRM1) and 817.5>113.1 *m/z* (MRM2) for DTX1, and 876.5>213.3 *m/z* (MRM1) and
169 876.5>823.5 *m/z* (MRM2) for PTX2. Calibration curves were performed in the range of 2 ng mL⁻¹

170 – 40 ng mL⁻¹ for OA and DTX1, and 5 ng mL⁻¹ – 50 ng mL⁻¹ for PTX2, at six calibration levels.
171 Calibration curve linearities were confirmed before and after each sample set. Curve correlation
172 coefficients (r^2) had to exceed 0.98 and slope deviations had to be below 25% to pursue toxin
173 quantifications. Limits of detection (LODs, signal/noise > 3) were 1.3 ng/mL for OA and DTX1,
174 and 1.7 ng/mL for PTX2. Limits of quantification (LOQs, signal/noise > 10) were 4 ng/mL for OA
175 and DTX1, and 5 ng/mL for PTX2. Samples were analyzed in duplicate.

176 **2.5. Statistical analysis**

177 Differences in toxin concentration (*i.e.*, OA and PTX2) among passive sampling disks (*i.e.*, β -CD-
178 HDI, β -CD-EPI, γ -CD-HDI, γ -CD-EPI and Diaion[®] HP-20), sampling points, and between weeks
179 were analyzed with analysis of variance (three-way ANOVA). In addition to P values, partial eta
180 squared (η_p^2) was used as a measure of effect size (*i.e.*, the importance of factors). Similar to r^2 ,
181 partial η_p^2 is the proportion of variation explained for a certain effect, and does not depend on
182 the number of sources of variation used in the ANOVA, thus it could be compared among
183 different designs (Tabachnick and Fidell, 2001). In contrast to P value, η_p^2 has the advantage of
184 allowing the proper comparison of treatments, whereas a lower P value does not necessarily
185 mean that a factor has stronger effect (see *e.g.*, Alcaraz et al., 2008). Adjusted (or marginal)
186 means of a dependent variables are the means for each level of the factor adjusted for the other
187 variables (see *e.g.*, Alcaraz et al., 2015), and were used to describe differences. Student's t test
188 was used to analyze differences in toxin concentration (OA vs. PTX2) for each passive sampling
189 disk. Quantitative variables were log-transformed prior to analysis because homoscedasticity
190 and linearity were clearly improved. All statistical analyses were performed with SPSS 26.0.

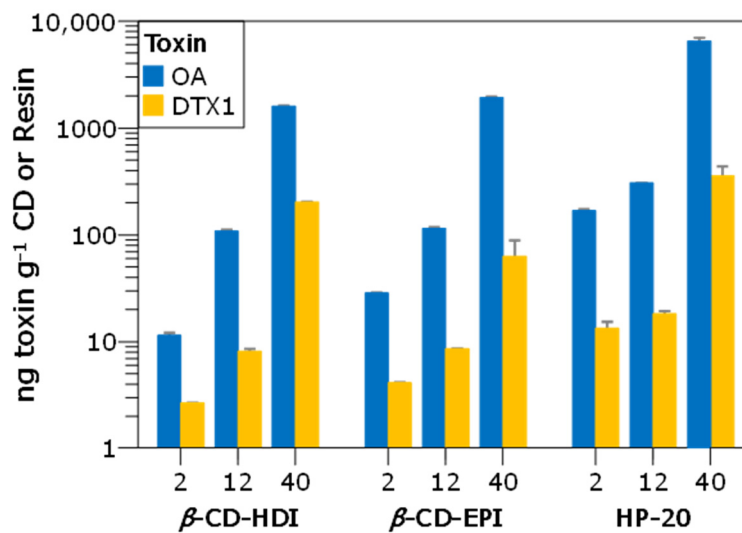
191

192

193 **3. Results**

194 **3.1. Analysis of cyclodextrins immersed in *Prorocentrum lima* cultures**

195 Toxins captured by β -CD-HDI, β -CD-EPI and Diaion® HP-20 immersed in *P. lima* cultures were
196 analyzed by LC-MS/MS, which revealed the presence of free OA and DTX1 in all of them (Fig. 2).
197 Although it is evident that Diaion® HP-20 provided the highest values, both cyclodextrins showed
198 OA and DTX1 capture. The OA contents at the different days were 7, 35 and 24% for β -CD-HDI
199 and 17, 38 and 30% for β -CD-EPI, compared to Diaion® HP-20. The DTX1 contents were 20, 44
200 and 56% for β -CD-HDI and 31, 47 and 17% for β -CD-EPI, compared to Diaion® HP-20. OA and
201 DTX1 contents showed exponential trends with culture day.

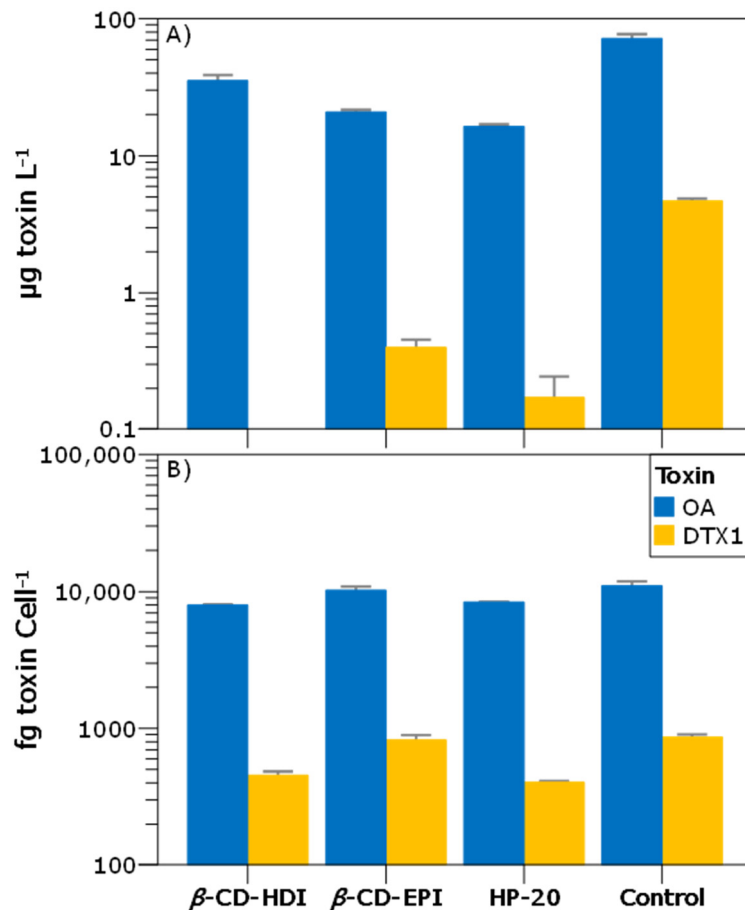


202

203 **Figure 2.** Free OA and DTX1 captured by the passive sampling disks immersed in *Prorocentrum lima*
204 cultures and collected at day 2, day 12 and day 40. Each bar corresponds to 1 disk analyzed twice.

205 *Prorocentrum lima* culture media and the corresponding microalgal cells at the moment of
206 harvesting were also analyzed (Fig. 3). The control culture, with neither cyclodextrins nor resin,
207 showed the highest toxin levels in the culture media. Nevertheless, it is interesting to mention
208 that the total number of cells at harvesting in the control culture was higher than in the cultures
209 with passive sampling disks, where the number of cells reached 54-65% that of the control
210 culture (Fig. 3S and Table 1S). The culture media with Diaion® HP-20 showed the lowest OA
211 contents (23% that of the control), followed by β -CD-EPI (29%) and finally β -CD-HDI (50%) (Fig.
212 3A), trend that was the opposite of that observed in the passive sampling materials (Fig. 2). Even

213 normalizing to the number of microalgal cells, the trend was the same. DTX1 contents were also
 214 lower in the culture media with Diaion® HP-20 than in the culture media with β -CD-EPI. However,
 215 this difference and the lack of DTX1 in the culture media with β -CD-HDI may be simply due to
 216 the fact that all DTX1 concentrations were very close to the LOD. When observing the toxin
 217 contents in the microalgal cells, no clear trends were observed (Fig. 3B).



218

219 **Figure 3.** Free OA and DTX1 present in the *P. lima* culture media (A) and in the microalgal cells (B) at day
 220 40.

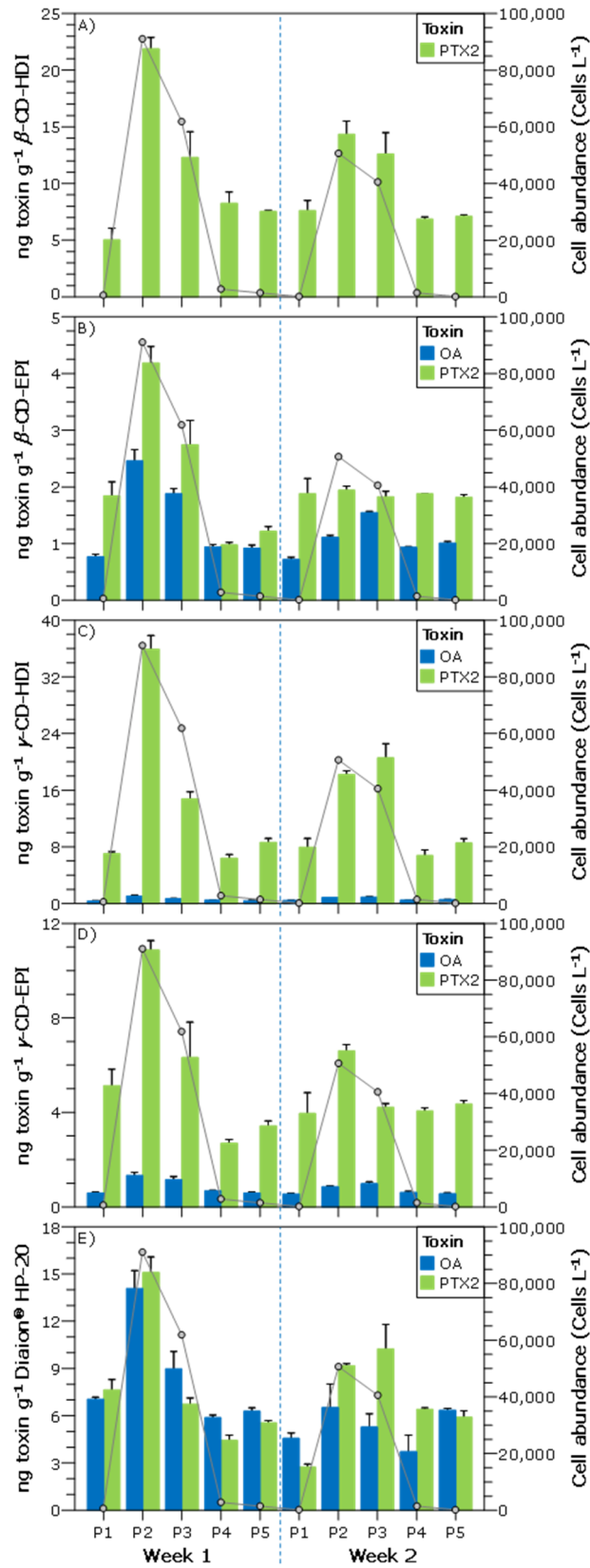
221 The analysis of hydrolyzed extracts showed fatty acid acyl OA esters in all cell pellets and small
 222 amounts of fatty acid acyl DTX1 esters in the cell pellets corresponding to the culture with β -CD-
 223 EPI (Fig. 4S). No esters were found in the culture media. Regarding the passive sampling disks,
 224 OA and DTX1 esters were detected in β -CD-EPI even after only 2 days, and OA esters were
 225 present in all cyclodextrins and the resin at the last sampling.

226 **3.2. Analysis of cyclodextrins deployed in a harbor during a *Dinophysis sacculus* bloom**

227 Toxins captured by β -CD-HDI, β -CD-EPI, γ -CD-HDI, γ -CD-EPI and Diaion® HP-20 deployed at 5
228 sampling points of El Masnou harbor (NW Mediterranean Sea) during two consecutive weeks of
229 a *D. sacculus* bloom were analyzed by LC-MS/MS. The analysis revealed the presence of OA and
230 PTX2 in all of them, sometimes at very different levels (Fig. 4, Fig. 5 and Fig. 6). Unlike the
231 experiment in *P. lima* cultures, DTX1 and esters were not found. It is important to mention that
232 although the LC-MS/MS analysis of extracts from β -CD-HDI revealed presence of OA, the
233 chromatographic peaks did not fulfil the analytical standard criteria and thus, quantification was
234 not possible. This effect was probably due to the presence of matrix compounds that interfere
235 in the analysis for this specific sampling material. Further work would be necessary to remove
236 this interference and quantify OA.

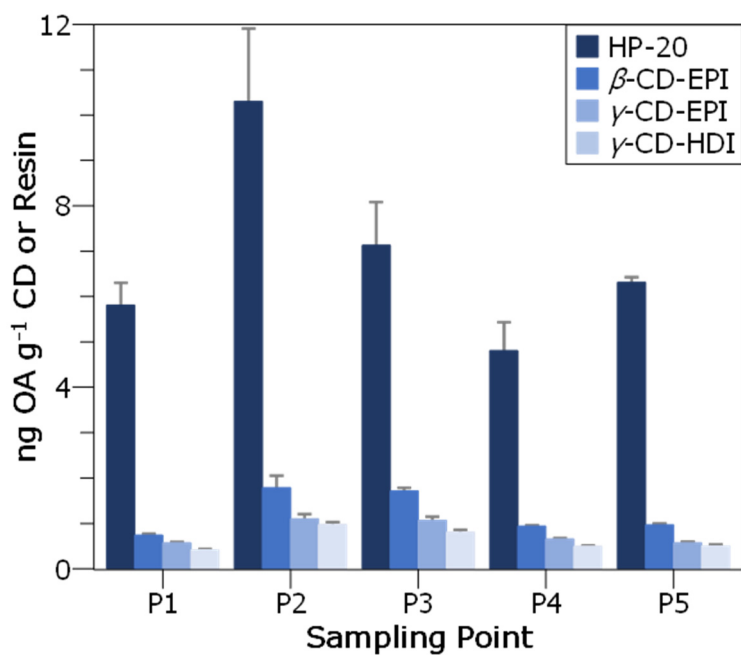
237 In general, considerable differences were observed between sampling points (ANOVA, $P < 0.0001$
238 for OA, and $P < 0.0001$ for PTX2, see Table 2S), P2 showing the highest toxin contents, followed
239 by P3, and with P1, P4 and P5 showing much lower toxin contents (Table 2S, Fig. 5S and 6S). This
240 trend is in accordance with the *D. sacculus* cell abundance distribution, which in the first
241 sampling week was 91,341 cells L⁻¹ in P2, 62,195 cells L⁻¹ in P3 and between 880 and 3,040 cells L⁻¹
242 in P1, P4 and P5. Additionally, in P2 and P3, toxin contents in sampling week 1 were higher than
243 in sampling week 2 (Table 2S, Fig. 7S and 8S), also following the temporal variation of *D. sacculus*
244 cell abundance, which decreased at the second deployment (e.g. to 50,949 cells L⁻¹ in P2 and
245 40,851 cells L⁻¹ in P3).

246 The global effect of type of cyclodextrin can be observed in Fig. 7, where data points have been
247 merged. In general terms, the trend for OA contents was Diaion > β -CD-EPI > γ -CD-EPI > γ -CD-
248 HDI and the trend for PTX2 contents was γ -CD-HDI > β -CD-HDI > Diaion > γ -CD-EPI > β -CD-EPI.
249 The OA contents were 17, 12 and 9% for β -CD-EPI, γ -CD-EPI and γ -CD-HDI, respectively,
250 compared to Diaion® HP-20. The PTX2 contents were 182, 144, 70 and 27% for γ -CD-HDI, β -CD-
251 HDI, γ -CD-EPI and β -CD-EPI, respectively, compared to Diaion® HP-20. Therefore, although
252 Diaion® HP-20 is better to capture OA, CD-HDIs are more efficient for PTX2.



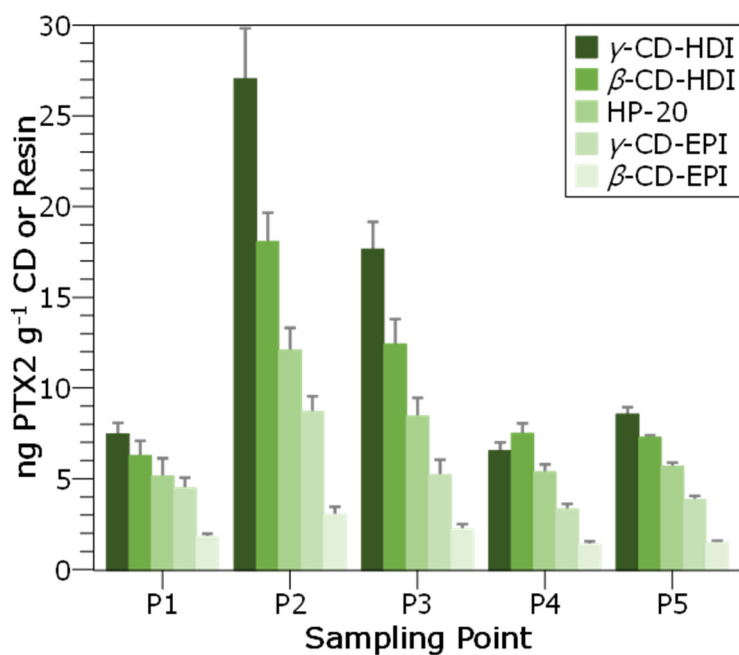
253

254 **Figure 4.** Left axis: OA and PTX2 captured by the passive sampling disks deployed El Masnou harbor (NW
 255 Mediterranean Sea). Right axis: *Dinophysis sacculus* cell abundance in the water column (average from
 256 deployment and collection days). Each bar corresponds to the mean of 2 disks (duplicates) analyzed
 257 twice.



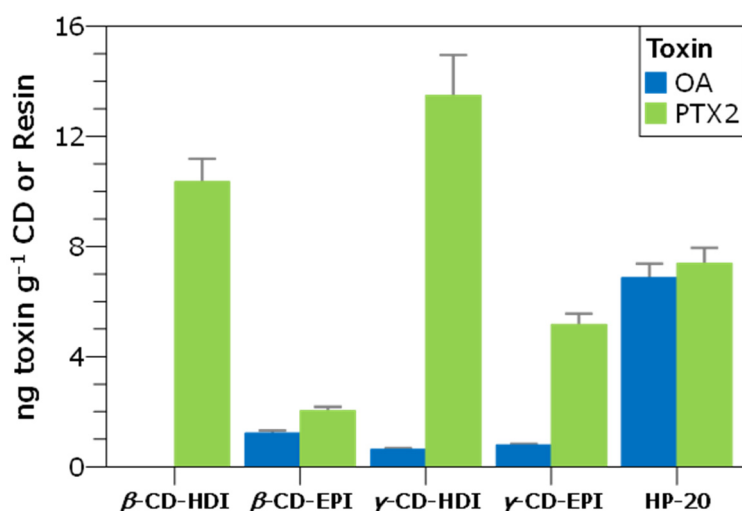
258

259 **Figure 5.** OA captured by the passive sampling disks per cyclodextrin/resin and sampling point (P1 to P5)
 260 of El Masnou harbor (NW Mediterranean Sea). Each bar corresponds to the mean of 4 disks (duplicates
 261 and 2 weeks) analyzed twice.



262

263 **Figure 6.** PTX2 captured by the passive sampling disks per cyclodextrin/resin and sampling point (P1 to
 264 P5) of El Masnou harbor (NW Mediterranean Sea). Each bar corresponds to the mean of 4 disks
 265 (duplicates and 2 weeks) analyzed twice.



266

267 **Figure 7.** Total OA and PTX2 captured by the passive sampling disks per cyclodextrin/resin deployed at El
 268 Masnou harbor (NW Mediterranean Sea). Each bar corresponds to the mean of 20 disks (duplicates, 2
 269 weeks and 5 points) analyzed twice. Error bars are the standard error of the means.

270

271 4. Discussion

272 4.1. Cyclodextrins immersed in *Prorocentrum lima* cultures

273 The immersion of β-CD-HDI, β-CD-EPI and Diaion® HP-20 in *P. lima* cultures for different days
 274 provided information about the toxin production of the strain combined with the toxin capture
 275 efficiency of the different passive sampling materials. LC-MS/MS analysis revealed the presence
 276 of OA and DTX1 in all extracts even at day 2 and, as expected, toxin contents showed an
 277 exponential increase trend with culture day. Although Diaion® HP-20 provided the highest toxin
 278 contents, both cyclodextrins also showed OA and DTX1 capture. Except for DTX1 at day 40, β-
 279 CD-EPI was slightly more efficient in capturing toxins than β-CD-HDI, and this observation was
 280 more evident at day 2 than at days 12 and 40, suggesting a faster capture rate of the former
 281 cyclodextrin. The percentage decrease of DTX1 in β-CD-EPI at day 40 (17%) could be due to
 282 different experimental parameters, such as a lower DTX1 production at that stage of the culture
 283 or the saturation of the passive sampling material. In general terms, although DTX1 values were
 284 around 10-fold lower than OA values, DTX1 capture with cyclodextrins was more efficient than
 285 OA capture compared to Diaion® HP-20. The additional methyl moiety in one of the extremes of

286 DTX1 (Fig. 9S) makes it less polar than OA, characteristic that could be favoring the interaction
287 with the cyclodextrins, as previously observed for Diaion® HP-20 (Li et al., 2011).

288 When making all these comparisons, it is important to keep in mind that β -CD-HDI, β -CD-EPI and
289 Diaion® HP-20 were immersed in different glass bottles during culture, in order to avoid
290 competition between them. Therefore, differences in microalgae growth and toxin composition
291 of the media cannot be discarded. Analysis of the culture media and the corresponding
292 microalgal cells contributed to better characterize the system. The analysis of *P. lima* culture
293 media at the moment of harvesting revealed lower dissolved toxin contents in the cultures with
294 passive sampling disks than in the control. However, the number of *P. lima* cells was also lower.
295 A possible explanation is that the presence of the disks may have inhibited the culture growth
296 (Table 1S), by decreasing light exposure or capturing culture media components (e.g. nutrients,
297 vitamins and metals). For those cultures with passive sampling disks, the trend of dissolved OA
298 content in the media was inversely proportional to that in the passive sampling material,
299 observation that supports the capture efficiency previously observed, which is Diaion® HP-20 >
300 β -CD-EPI > β -CD-HDI. Regarding the toxin contents in microalgal cells, no clear trends were
301 observed among passive sampling materials and no significant differences with the control. This
302 seems to indicate that the passive sampling disks, although are affecting culture growth, may
303 not be affecting toxin production per cell.

304 Regarding to absolute values and compared to other works, much lower toxin contents are
305 obtained herein (e.g. 168 ng OA g⁻¹ and 13 ng DTX1 g⁻¹ for the Diaion® HP-20 after 48 h in front
306 of 982 ng OA g⁻¹ and 846 ng DTX1 g⁻¹ found by Fux et al., 2008), differences probably due to the
307 strain, its age and the culture experimental conditions.

308 *Prorocentrum lima* is a well-known producer of OA, DTX1, DTX2 and several types of esters, the
309 toxin profile and contents depending on the strain and growing conditions (Pan et al., 1999,
310 Bravo et al., 2001, Nascimento et al., 2005, Paz et al., 2007, Morton et al., 2009, Vale et al., 2009,

311 Li et al., 2012, Hu et al., 2017). However, no esters or only trace amounts are usually found in
312 culture media (Pan et al., 1999, Nascimento et al., 2005), probably because they are hydrolyzed
313 before their release from the cells (Hu et al., 2017). In the current work, esters were not found
314 in the culture media either. Regarding their presence in passive samplers, a previous work
315 showed that OA esters were detected in SPATT bags with Diaion® HP-20 (Mackenzie et al., 2011).
316 In the current work, OA and DTX1 esters were detected in some passive sampling disks, mainly
317 in those from the last sampling. The lipophilic character of the fatty acid acyl ester derivatives
318 makes them suitable to be captured by the cyclodextrins and the Diaion® HP-20 resin. Therefore,
319 these passive sampling materials could be pre-concentrating esters once released from the cells,
320 allowing their detection better than in the media.

321 **4.2 Cyclodextrins deployed in a harbor during a *Dinophysis sacculus* bloom**

322 The deployment of β -CD-HDI, β -CD-EPI, γ -CD-HDI, γ -CD-EPI and Diaion® HP-20 passive samplers
323 during a *D. sacculus* bloom revealed the capture of OA and PTX2. However, there is not a clear
324 indication about which was the most predominant toxin, since different passive sampling
325 materials provide different trends (Fig. 4). Additionally, in the current work, toxin levels in the
326 cyclodextrins (or in the commercial resin used as a control) did not reach the values found in
327 other works, which may suggest an overall lower toxin production from the bloom. The toxin
328 concentration and profile of *D. sacculus* may vary depending on the strain, its geographical
329 origin, the experimental parameters of the culture and, of course, multiple environmental
330 conditions in the case of field samples. In the Mediterranean, *D. sacculus* blooms have been
331 associated to OA (Cañete et al., 2008; Garibo et al., 2014; García-Altare et al., 2016; Leonardo
332 et al., 2018; Giacobbe et al., 2000), PTX2 (Cañete et al., 2008; García-Altare et al., 2016; and
333 sometimes DTX1, to a lesser extent (Giacobbe et al., 2000). In a previous study performed by our
334 group during a *D. sacculus* bloom in Alfacs Bay (NW Mediterranean Sea), 200 km to the south of
335 Masnou harbor, PTX2 was the main component in the toxin profiles of phytoplankton aggregates
336 (up to 668 pg PTX2 cell⁻¹ in front of 461 pg OA cell⁻¹), while OA was the most concentrated toxin

337 in Diaion® HP-20 SPATTs (94 ng OA g⁻¹ in front of 42 ng PTX2 g⁻¹) (García-Altarets et al., 2016). In
338 another work performed with a culture of a *D. sacculus* strain from Galicia (NE Atlantic Ocean),
339 PTX2 was also the main toxin in the cells (13 pg cell⁻¹), followed by OA (8 pg cell⁻¹), whereas OA
340 was more abundant in the medium (28 ng OA mL⁻¹ in front of 23 ng PTX2 mL⁻¹) (Riobó et al.,
341 2013). In that work, only traces of DTX1 were observed in the cell pellet extract, but not in the
342 medium. OA contents in SPATT discs deployed during a *D. acuta* event in the west coast of Ireland
343 (Atlantic Ocean) were also much higher than PTX2, followed by DTX2 (maximum of 5645 ng OA g⁻¹,
344 1265 ng PTX2 g⁻¹ and 533 ng DTX2 g⁻¹) (Fux et al., 2009). The deployment of passive samplers
345 in Galicia (NE Atlantic Ocean) during a bloom where several *Dinophysis* species were present
346 (mainly *D. ovum* and *D. acuminata*, but also *D. acuta* and *D. caudata*, depending on the day) also
347 followed this pattern (maximum 4495 ng OA g⁻¹, 2705 ng PTX2 g⁻¹ and 1876 ng DTX2 g⁻¹) (Pizarro
348 et al., 2013). On the contrary, toxin contents found in SPATT discs deployed during another
349 *D. acuta* bloom near the south-west coast of Ireland (Atlantic Ocean) were higher for PTX2
350 (between 1.1 and 4.5 µg g⁻¹), followed by DTX2 (between 0.9 and 3.7 µg g⁻¹) and finally OA
351 (between 0.8 and 2.9 µg g⁻¹) (Fux et al., 2010), and the deployment of SPATT bags during a
352 *D. acuminata* bloom in New Zealand also resulted in higher levels of PTX2 compared to OA and
353 DTX1, which were 1.73 µg PTX2 g⁻¹ and 0.11 µg OA/DTX1 g⁻¹ when the maximum cell numbers of
354 *D. acuminata* were observed. All these works underline the complexity in the understanding and
355 elucidation of toxin profiles.

356 Nevertheless, results provided herein showed interesting and informative trends. Regarding
357 location distribution, the highest toxin contents, for both OA and PTX2, were detected in the
358 sampling points with the highest *D. sacculus* cell abundance (Fig. 4). When looking at the
359 geographical position of the sampling points (Fig. 2S), P2 is in an interior corner of the harbor,
360 followed by P3, and finally by P4, P5 and P1. Thus, a correlation with the spatial *D. sacculus*
361 bloom dynamics is observed, *D. sacculus* cells accumulating in the most confined part of the
362 harbor. Additionally, apart from the *D. sacculus* cell abundance, the diffusion of the dissolved

363 toxins may be playing a role. Regarding temporal distribution, data from P2 and P3 clearly
364 demonstrate that toxin contents correlate with the temporal variation of *D. sacculus* cell
365 abundance. Another important issue is that OA and PTX2 were detected in almost all samples,
366 even at very low *D. sacculus* cell abundances (as low as 400 cells L⁻¹), which indicated how
367 common traces of these toxins are in seawater and how stable they are (already demonstrated
368 at least for OA, Blanco et al., 2018), and also how sensitive the SPATT strategy is.

369 It is evident that PTX2 capture with cyclodextrins was more efficient than OA capture (Fig. 7).
370 This can be explained considering the structures of both toxins and cyclodextrin polymers and
371 the interactions involved in the capture process. The Diaion® HP-20 resin is known to capture a
372 wide range of organic molecules from aqueous solution through a hydrophobic binding
373 mechanism involving its styrene-divinylbenzene matrix. That is why it showed no significantly
374 different OA and PTX2 contents (Student's *t*-test, *P* = 0.53) and is not selective to any of the toxins
375 as compared with the cyclodextrin-based materials that show higher contents for PTX2
376 (Student's *t*-test, *P* < 0.0001 in all cases). Unlike OA and DTX1, OA and PTX2 have very different
377 structures with different overall hydrophilic/hydrophobic balances (Fig. 9S). PTX2 is a neutral
378 molecule with a ring structure composed by oxolane and oxane rings connected by aliphatic
379 spacers (O'Rourke et al., 2017). This makes PTX2 a polar but essentially hydrophobic molecule,
380 which could favor its capture by cyclodextrins and may explain the higher capture efficiency of
381 the cyclodextrin polymers over Diaion® HP-20. On the other hand, OA is also composed by
382 oxolane and oxane rings but in a linear structure and possesses an ionizable carboxylic acid group
383 at the A ring resulting in a higher polarity and solubility in aqueous solution (Mackenzie et al.,
384 2004). This may explain, in general terms, its lower capture by the cyclodextrins as compared to
385 the commercial resin.

386 In the case of the cyclodextrin materials, their capture efficiency should be a combination of the
387 cavity size and the nature of the bridging units. Regarding OA and cavity size, capture efficiencies
388 with β-CD-EPI, consisting of seven glucopyranose units, were only slightly higher (Table 2S and

389 Fig. 10S) than with γ -CD-EPI, consisting of eight glucopyranose units (it is important to mention
390 that absolute OA contents were in general very low). Therefore, the cavity size plays a negligible
391 effect, if any, in the capture process of OA. Nevertheless, when looking at the PTX2 results, γ -CD-
392 HDI and γ -CD-EPI provided significantly higher capture efficiencies than their β -CD counterparts
393 (Table 2S and Fig. 11S), suggesting that the larger internal diameter (0.95 nm for γ -CDs in front
394 of 0.78 nm for β -CDs (Szejtli, 1998)) could be playing a role in accommodating the PTX2 molecule,
395 most likely through the D/E rings.

396 On the other hand, the role of the bridging units was more evident in the case of PTX2 than OA.
397 Both CD-EPIs, which contain polar hydroxyalkyl groups of different lengths depending on the
398 degree of polymerization, were slightly more efficient than CD-HDI in capturing the more polar
399 OA (Table 2S and Fig. 10S). On the contrary, CD-HDIs were much more efficient in capturing the
400 more lipophilic PTX2 than CD-EPIs (Table 2S and Fig. 11S). The explanation could rely on the
401 higher hydrophobicity of the HDI spacer (which contains six CH₂ groups connected to the CD by
402 O(C=O)NH groups) compared to EPI that provides a more hydrophobic environment for PTX2, as
403 well as the occurrence of hydrogen bond interactions between the amido and OH groups of the
404 capture polymer with the polar groups of the toxin. Therefore, the nature of the bridging units
405 is certainly playing a more decisive role than the cavity size in this case as evidenced by the trend
406 γ -CD-HDI > β -CD-HDI > Diaion > γ -CD-EPI > β -CD-EPI. Another important point to consider is that,
407 in contrast to Diaion® HP-20, γ -CD-HDI and β -CD-HDI are not porous materials and the capture
408 of PTX2 occurs mainly on the surface of the particles. Hence, the high capture efficiency showed
409 by materials with a lower active surface such as both cyclodextrin polymers is indicative of the
410 high strength of the intermolecular interactions involved.

411 An experiment was performed in the lab, with seawater spiked with the two toxins at equimolar
412 concentrations, to investigate if competition of OA and PTX2 for the cyclodextrin cavities could
413 explain the results obtained in the *in-situ* deployment experiment. However, all cyclodextrins
414 were able to capture both toxins with recovery values of about 80%, and no competition was

415 observed. In fact, although the saturation of the cyclodextrins was not evaluated, it is evident
416 that toxin contents in the cyclodextrins from the *in-situ* deployment experiment were far from
417 saturation (much lower toxin contents than those reached in the culture experiment). Thus, what
418 is happening in nature is much more complex and other environmental parameters are certainly
419 playing a significant role. Since cyclodextrins are not specific for marine toxins, capture and
420 competition of other compounds from seawater (e.g. chemical contaminants, organic matter,
421 micro/nanoplastics and demucilaged seeds) cannot be discarded.

422 **4.3 General discussion**

423 The cyclodextrin-based materials tested in this work have provided useful information regarding
424 the toxin profile of a *P. lima* strain and the spatial and temporal dynamics of a *D. sacculus* bloom.
425 It is necessary to take into account that these passive sampling materials are capturing dissolved
426 toxins from the culture media or the seawater, during a time interval, and with different
427 efficiencies. Therefore, as observed in this work, discrepancies may arise among them. Although
428 more work is required to better understand the results and to fully characterize the two case
429 studies, multiple experimental parameters are not under control (e.g. diffusion of dissolved
430 toxins, competition of toxins with other compounds that can also be captured by cyclodextrins,
431 stability of dissolved toxins, environmental conditions, etc.). Nevertheless, this work is a step
432 forward to understand what is happening in nature.

433 Compared to other passive sampling materials, cyclodextrins have the advantages of being easy
434 to manufacture, cheap and ecologically sustainable, and their chemical and structural versatility
435 could allow a rational synthesis according to the type of toxin to be captured. Therefore, they
436 could be useful as early warning tools in monitoring programs. To this purpose, toxin contents in
437 shellfish from specific regions should be determined, tailor-made cyclodextrins should be tested,
438 and correlation between both should be established.

439

440 **5. Conclusions**

441 Summarizing, the results of the experiments described herein demonstrate the potential of
442 cyclodextrin polymers as new materials for passive sampling of lipophilic marine toxins. In the
443 culture experiment, OA and DTX1, and related esters at a lower extent, have been captured along
444 *P. lima* culture time, the first signals being detected even after only 2 days. In the *in-situ*
445 deployment experiment, toxin contents were significantly higher in the sampling points and
446 dates where *D. sacculus* cell abundance was also higher, the effect being more evident for PTX2
447 than for OA. While the exact capture mechanism and the role of cavities and spacers is currently
448 under study, the evaluated cyclodextrin-based materials have already proven efficient in
449 providing integrated contents of toxins released into culture media and the environment. Further
450 investigation is underway to evaluate the capture and equilibrium rates, saturation, regeneration
451 and reusability, to remove matrix effects and to establish the correlations with shellfish
452 contamination with the aim to develop novel passive sampling materials able to satisfy the
453 environmental monitoring demands of specific geographic regions.

454 **Sample CRediT author statement**

455 **Mònica Campàs:** Conceptualization, Methodology, Investigation, Resources, Writing - original
456 draft, Writing - review & editing, Supervision, Project administration, Funding acquisition. **Maria**
457 **Rambla-Alegre:** Methodology, Investigation, Writing - review & editing. **Charlotta Wirén:**
458 Investigation, Formal Analysis, Writing - review & editing. **Carles Alcaraz:** Formal Analysis,
459 Visualization, Writing - review & editing. **María Rey:** Methodology, Investigation, Writing - review
460 & editing. **Anna Safont:** Investigation, Writing - review & editing. **Jorge Diogène:** Methodology,
461 Writing - review & editing. **Mabel Torréns:** Resources, Writing - review & editing. **Alex Fragoso:**
462 Conceptualization, Resources, Writing - review & editing, Project administration, Funding
463 acquisition.

464 **References**

465 Alcaraz, C., Pou-Rovira, Q., García-Berthou, E., 2008. Use of a flooded salt marsh habitat by an
466 endangered cyprinodontid fish (*Aphanius iberus*). *Hydrobiologia* 600, 177–185.

467 Alcaraz, C., Gholami, Z., Esmaeili, H.R., García-Berthou, E., 2015. Herbivory and seasonal changes
468 in diet of a highly endemic cyprinodontid fish (*Aphanius farsicus*). *Environ. Biol. Fishes* 98, 1541–
469 1554.

470 Blanco, J., Martín-Morales, E., Álvarez, G., 2018. Stability of okadaic acid and 13-desmethyl
471 spirolide C in seawater and sediment. *Mar. Chem.* 207, 21–25.

472 Bravo, I., Fernández, M.L., Ramilo, I., Martínez, A., 2001. Toxin composition of the toxic
473 dinoflagellate *Prorocentrum lima* isolated from different locations along the Galician coast (NW
474 Spain). *Toxicon* 39, 1537–1545.

475 Cañete, E., Caillaud, A., Fernández, M., Mallat, E., Blanco, J., Diogène, J., 2008. *Dinophysis*
476 *sacculus* from Alfacs Bay, NW Mediterranean. Toxin profiles and cytotoxic potential, in:
477 Proceedings of the 12th International Conference on Harmful Algae, International Society for
478 the Study of Harmful Algae and Intergovernmental Oceanographic Commission of UNESCO,
479 Copenhagen, pp. 279–281.

480 Crini, G., Cosentino, C., Bertini, S., Naggi, A.M., Torri, G., Vecchi, C., Janus, L., Morcellet, M., 1998.
481 Solid-state NMR spectroscopy study of molecular motion in cyclomaltopeptaose (β -
482 cyclodextrin) crosslinked with epichlorohydrin. *Carbohydr. Res.* 308, 37–45.

483 Fux, E., Marcaillou, C., Mondeguer, F., Bire, R., Hess, P., 2008. Field and mesocosm trials on
484 passive sampling for the study of adsorption and desorption behaviour of lipophilic toxins with
485 a focus on OA and DTX1. *Harmful Algae* 7, 574–583.

486 Fux, E., Bire, R., Hess, P., 2009. Comparative accumulation and composition of lipophilic marine
487 biotoxins in passive samplers and in mussels (*M. edulis*) on the West Coast of Ireland. *Harmful*
488 *Algae* 8, 523–537.

489 Fux, E., González-Gil, S., Lunven, M., Gentien, P., Hess, P., 2010. Production of diarrhetic shellfish
490 poisoning toxins and pectenotoxins at depths within and below the euphotic zone. *Toxicon* 56,
491 1487–1496.

492 García-Altare, M., Casanova, A., Fernández-Tejedor, M., Diogène, J., de la Iglesia, P., 2016.
493 Bloom of *Dinophysis* spp. dominated by *D. sacculus* and its related diarrhetic shellfish poisoning
494 (DSP) outbreak in Alfacs Bay (Catalonia, NW Mediterranean Sea): identification of DSP toxins in
495 phytoplankton, shellfish and passive samplers. *Regional Stud. Mar. Sci.* 6, 19–28.

496 Garibo, D., Campbell, K., Casanova, A., de la Iglesia, P., Fernández-Tejedor, M., Diogène, J.,
497 Elliott, C.T., Campàs M., 2014. SPR immunosensor for the detection of okadaic acid in mussels
498 using magnetic particles as antibody carriers. *Sens. Actuators B-Chem.* 190, 822–828.

499 Giacobbe, M. G., Penna, A., Ceredi, A. Milandri, A., Poletti, R., Yang, X., 2000. Toxicity and
500 ribosomal DNA of the dinoflagellate *Dinophysis sacculus* (Dinophyta). *Phycologia* 39, 177–182.

501 Hu, T., LeBlanc, P., Burton, I.W., Walter, J.A., McCarron, P., Melanson, J.E., Strangman, W.K.,
502 Wright, J.L.C., 2017. Sulfated diesters of okadaic acid and DTX-1: Self-protective precursors of
503 diarrhetic shellfish poisoning (DSP) toxins. *Harmful Algae* 63, 85–93.

504 Kudela, R.M., 2017. Passive sampling for freshwater and marine algal toxins. In: *Recent advances*
505 *in the analysis of marine toxins*; Diogène, J., Campàs, M., Eds.; Elsevier: Netherlands, 2017;
506 *Comprehensive Analytical Chemistry*, Vol. 78, pp 379–409.

507 Leonardo, S., Toldrà, A., Rambla-Alegre, M., Fernández-Tejedor, M., Andree, K.B., Ferreres, L.,
508 Campbell, K., Elliott, C.T., O'Sullivan, C., Pazos, Y., Diogène, J., Campàs, M., 2018. Self-assembled
509 monolayer-based immunoassays for okadaic acid detection in seawater as monitoring tools.
510 *Mar. Environ. Res.* 133, 6–14.

511 Li, A., Ma, F., Song, X., Yu, R., 2011. Dynamic adsorption of diarrhetic shellfish poisoning (DSP)
512 toxins in passive sampling relates to pore size distribution of aromatic adsorbent. *J. Chromatogr.*
513 *A* 1218, 1437–1442.

514 Li, J., Li, M., Pan, J., Liang, J., Zhou, Y., Wu, J., 2012. Identification of the okadaic acid-based toxin
515 profile of a marine dinoflagellate strain *Prorocentrum lima* by LC–MS/MS and NMR
516 spectroscopic data. *J. Sep. Sci.* 35, 782–789.

517 MacKenzie, L., Beuzenberg, V., Holland, P., McNabb, P., Selwood, A., 2004. Solid phase
518 adsorption toxin tracking (SPATT): a new monitoring tool that simulates the biotoxin
519 contamination of filter feeding bivalves. *Toxicon* 44 901–918.

520 MacKenzie, L., Selwood, A., McNabb, P., Rhodes, L., 2011. Solid phase adsorption toxin tracking
521 (SPATT): a new monitoring tool that simulates the biotoxin contamination of filter feeding
522 bivalves. *Harmful Algae* 10, 559–566.

523 Mohamed, M.H., Wilson, L. D., Headley, J.V., 2011. Design and characterization of novel β -
524 cyclodextrin based copolymer materials. *Carbohydr. Res.* 346, 219–229.

525 Morton, S.L., Vershinin, A., Smith, L.L., Leighfield, T.A., Pankov, S., Quilliam, M.A., 2009.
526 Seasonality of *Dinophysis* spp. and *Prorocentrum lima* in Black Sea phytoplankton and associated
527 shellfish toxicity. *Harmful Algae* 8, 629–636.

528 Nascimento, S.M., Purdie, D.A., Morris, S., 2005. Morphology, toxin composition and pigment
529 content of *Prorocentrum lima* strains isolated from a coastal lagoon in southern UK. *Toxicon* 45,
530 633–649.

531 O'Rourke, N.F., A, M., Higgs, H.N., Eastman, A., Micalizio, G.C., 2017. Function-oriented studies
532 targeting pectenotoxin 2: synthesis of the GH-ring system and a structurally simplified
533 macrolactone. *Org. Lett.* 19, 5154–5157.

534 Ortiz, M., Fragoso, A., O'Sullivan, C.K., 2011. Amperometric detection of antibodies in serum:
535 performance of self-assembled cyclodextrin/cellulose polymer interfaces as antigen carriers.
536 *Org. Biomol. Chem.* 9, 4770–4773.

537 Ortiz, M., Fragoso, A., O'Sullivan, C.K., 2011. Detection of antigliadin autoantibodies in celiac
538 patient samples using a cyclodextrin-based supramolecular biosensor. *Anal. Chem.* 83, 8, 2931–
539 2938.

540 Ortiz, M., Torrens, M., Alakulppi, N., Strömbom, L., Fragoso, A., O'Sullivan, C.K., 2011.
541 Amperometric supramolecular genosensor self-assembled on cyclodextrin-modified surfaces.
542 *Electrochem. Commun.* 13, 578–581.

543 Ortiz, M., Torrens, M., Canela, N., Fragoso, A., O'Sullivan, C.K., 2011. Supramolecular
544 confinement of polymeric electron transfer mediator on gold surface for picomolar detection of
545 DNA. *Soft Matter*. 7, 10925–10930.

546 Ortiz, M., Wajs, E.M., Fragoso, A., O'Sullivan, C.K., 2012. A bienzymatic amperometric
547 immunosensor exploiting supramolecular construction for ultrasensitive protein detection.
548 *Chem. Commun.* 48, 1045–1047.

549 Ortiz, M., Wilson, L., Botero, M.L., Baker, P., Iwuoha, E., Fragoso, A., O'Sullivan, C.K., 2014.
550 Supramolecular amperometric immunosensor for detection of human chorionic gonadotropin.
551 *Electroanal.* 26, 1481–1487.

552 Pan, Y., Cembella, A. D., Quilliam, M. A., 1999. Cell cycle and toxin production in the benthic
553 dinoflagellate *Prorocentrum lima*. *Mar. Biol.* 134, 54–549.

554 Paz, B., Daranas, A.H., G. Cruz, P.G., Franco, J.M., Pizarro, G., Souto, M.L., Norte, M., Fernández,
555 J.J., 2007. Characterisation of okadaic acid related toxins by liquid chromatography coupled with
556 mass spectrometry. *Toxicon* 50, 225–235.

557 Pizarro, G., Moroño, Á., Paz, B., Franco, J.M., Pazos, Y., Reguera B., 2013. Evaluation of passive
558 samplers as a monitoring tool for early warning of *Dinophysis* toxins in shellfish. *Mar. Drugs* 11,
559 3823–3845.

560 Provasoli, L., 1968. Media and Prospects for the Cultivation of Marine Algae, in: Cultures and
561 collection of algae, Proceedings of the US-Japanese conference, Japan Society of Plant
562 Physiology, Hakone, pp. 63–75.

563 Ramirez, H.L., Cao, R., Fragoso, A., Torres-Labandeira, J.J., Dominguez, A., Schacht, E.H., Baños,
564 M., Villalonga, R., 2006. Improved anti-inflammatory properties for naproxen with cyclodextrin-
565 grafted polysaccharides. *Macromol. Biosci.* 6, 555–561.

566 Ramirez, H.L., Valdivia, A., Cao, R., Torres-Labandeira, J.J., Fragoso, A., Villalonga, R. 2006.
567 Cyclodextrin-grafted polysaccharides as supramolecular carrier systems for naproxen.
568 *Bioorganic Med. Chem. Let.* 16, 1499–1501.

569 Ramirez, H.L., Valdivia, A., Cao, R., Fragoso, A., Torres-Labandeira, J.J., Baños, M., Villalonga, R.,
570 2007. Preparation of beta-cyclodextrin-dextran polymers and their use as supramolecular
571 carrier systems for naproxen. *Polym. Bull.* 59, 597–605.

572 Riobó, P., Reguera, B., Franco, J. M., Rodríguez, F., 2013. First report of the toxin profile of
573 *Dinophysis sacculus* Stein from LC–MS analysis of laboratory cultures. *Toxicon* 76, 221–224.

574 Roué, M., Darius, H.T., Chinain, M., 2018. Solid phase adsorption toxin tracking (SPATT)
575 technology for the monitoring of aquatic toxins: a review. *Toxins* 10, 167.

576 Szejtli, J., 1998. Introduction and General Overview of Cyclodextrin Chemistry, *Chem. Rev.* 98,
577 1743–1754.

578 Tabachnick, B.G., Fidell, L.S., 2001. *Computer-Assisted Research Design and Analysis*, 1st ed.
579 Allyn & Bacon, Inc., USA.

580 Utermöhl, V.H., 1931. Neue Wege in der quantitativen erfassung des planktons. (Mit besondere
581 Berücksichtigung des Ultraplanktons). *Verhandlungen Int. Ver. Für Theoretische Angew. Limnol.*
582 5, 567–595.

583 Vale, P., Veloso, V., Amorim, A., 2009. Toxin composition of a *Prorocentrum lima* strain isolated
584 from the Portuguese coast. *Toxicon* 54, 145–152.

585 Vilallonga, R., Cao, R., Fragoso, A., 2007. Supramolecular chemistry of cyclodextrins in enzyme
586 technology. *Chem. Rev.* 107, 3088–3116.

587 Wajs, E.M., Caldera, F., Trotta, F., Fragoso, A., 2014. Peroxidase-encapsulated cyclodextrin
588 nanosponge immunoconjugates as a signal enhancement tool in optical and electrochemical
589 assays. *Analyst* 13, 375–380.

590 Wajs, E.M., Fernandez, N., Fragoso, A., 2016. Supramolecular biosensors based on
591 electropolymerised pyrrole-cyclodextrin modified surfaces for antibody detection. *Analyst* 141,
592 3274–3279.

593 Wells, M.L., Karlson, B., Wulff, A., Kudela, R., Trick, C., Asnaghi, V., Berdalet, E., Cochlan, W.,
594 Davidson, K., De Rijcke, M., Dutkiewicz, S., Hallegraeff, G., Flynn, K.J., Legrand, C., Paerl, H., Silke,
595 J., Suikkanen, S., Thompson, P., Trainer, V.L., 2020. Future HAB science: Directions and
596 challenges in a changing climate. *Harmful Algae* 91, 101632.

597 Zendong, Z., McCarron, P., Herrenknecht, C., Sibat, M., Amzil, Z., Cole, R.B., Hess, P., 2015. High
598 resolution mass spectrometry for quantitative analysis and untargeted screening of algal toxins
599 in mussels and passive samplers. *J. Chromatogr. A* 1416, 10–21.

600 **Acknowledgments**

601 The research has received funding from the Ministerio de Ciencia, Innovación y Universidades
602 (MICINN), the Agencia Estatal de Investigación (AEI) and the Fondo Europeo de Desarrollo
603 Regional (FEDER) through the CIGUASENSING (BIO2017-87946-C2-1-R and BIO2017-87946-C2-
604 2-R) and CELLECTRA (PID2020-112976RB-C21 and PID2020-112976RB-C22) projects. The
605 authors acknowledge support from CERCA Programme/Generalitat de Catalunya. Charlotta
606 Wirén acknowledges support from the Master's Degree in Zoonosis and One Health from the

607 Universitat Autònoma de Barcelona. The authors also acknowledge Vanessa Castan, José Luis
608 Costa, Esther Dàmaso, Laura Ferreres, Lluís Jornet and Sandra Leonardo for the technical work.